

Received Signal Strength Based Wireless Source Localization with Inexact Anchor Position

Yang Liu

Abstract—Received signal strength(RSS)-based approach of wireless localization is easy to implement at low cost. In practice, exact positions of anchors may not be available. This paper focuses on determining the location of the source in the presence of inexact position of anchors based on RSS directly. This study at first uses Taylor expansion and a min-max approach to get the approximate maximum likelihood estimator of the source coordinates. Then this paper proposes a relaxed semi-definite programming model to circumvent the non-convexity. This paper also proposes a rounding algorithm concerning both the inexact source location and the inaccurate anchor location. Experimental results together with analysis are presented to validate the proposed method

Index Terms—Robust Source Localization; Received Signal Strength; Semidefinite Programming; Inexact Anchor Position

I. INTRODUCTION

SOURCE wireless localization is a significant problem encountered in many indoor and outdoor applications, including cyber-physical systems, health, environment monitoring, home, and office automation, weather forecasting, and so on. Although GPS is a simple solution, the high cost and power consumption, and poor performance inside an indoor environment have necessitated the research on other localization methods.

In wireless localization, there are some nodes equipped with wireless transmission and reception devices, and with already known location information. These type of nodes are anchors. It is necessary to have some measurements related to the source and anchors in a localization procedure. These measurements include, for example, Time of Arrival(TOA), Angle of Arrival(AOA), and Received Signal Strength(RSS). Because of its implementation simplicity, RSS technology gradually becomes the primary concern.

Given measurements information, the localization procedure can always be formed as a maximum likelihood (ML) estimation problem. That is, the localize algorithm at first re-express the joint probability of the sample data (measurements) as a likelihood function that treats the source coordinates x as a variable, and evaluated at the observed measurement sample. Next is thus to find the supremum value of the likelihood function by choice of x .

The maximum likelihood objective function can be quite different when the model changes(measurement type and

system uncertainty). Due to the nature of the localization problem itself, the ML estimator for localization is always nonconvex and nonlinear, so that to solve the original problem have limited success even for small problem size. Generally speaking, applying a various degree of relaxation to the original problem is always necessary.

Most research works assume that the exact positions of anchors are known. However, in reality, this assumption often is too strong. Neglecting the inaccuracy of anchor position will undoubtedly deteriorate the localization performance severely. The production of the localization algorithm will also be influenced by the measurement noise and the number of anchors. The localization algorithm should be 'robust' to overcome the anchor location uncertainty and measurement noise.

This paper model the inaccuracy of the anchors as a bounded random vector. A robust method dealing with the error of the anchors is proposed adopting RSS measurement directly. At first, this paper proposes a maximum likelihood nonconvex model based on RSS. This model takes into account the location error of anchors. Then this paper transforms and relaxes the original to an SDR (Semidefinite Programming Relaxation) problem, which is convex and easy to solve. Cramer-Rao Lower Bound(CRLB) as a performance benchmark of the proposed estimator and the number of times needs of Monte Carlo method are also derived. A rounding algorithm is proposed, considering both the inaccuracy of anchors and the source location at the same time. Simulation results show that the proposed SDP based estimator plus rounding method outperform all other techniques that we compared. It should be mention here that the source localization problem(or it's variants) has been studied in various contexts before. However, these earlier works have quite different emphases from this paper. To the best of our knowledge, this is the first work considering the inaccurate anchors in the only RSS measurement scenario. And the rounding method is also first put forward.

The contribution of this paper is highlighted as follows:

- For the case of simple RSS measurement-based localization with inaccurate anchors, this paper firstly proposes a relaxed solvable estimator.
- This paper analyzes different problem-dependent rounding strategies. Then this paper firstly proposes a rounding algorithm considering inaccurate anchors and non-feasible source location simultaneously.
- This paper gives the procedure of calculating the minimum number of Monte Carlo simulation trials needed. This paper also derives the Cramer-Rao lower bound of the proposed estimator considering anchor's position error.

Yang Liu is with the School of Information Engineering, Guangdong University of Technology, Guangzhou China, (email:liuyang@gdut.edu.cn). This work has been submitted to the IEEE for possible publication. Copyright may be transferred without notice, after which this version may no longer be accessible.

The paper is organized as follows. Section II examined related works. Section III describes the basic idea and details of the proposed convex estimator for source localization using RSS with inaccurate anchor locations. This section also analyzes different rounding strategies. Section V presents numerical results and analysis for the proposed localization methods comparing with other methods elaborately. Finally, some concluding remarks and future research suggestions are given in Section VI. Appendix A derives the experiment times needed for the Monte Carlo simulation. Appendix B gives the CRLB of our model as a performance benchmark.

II. RELATED WORKS

There has been a rich history of published works that attempt to solve the source localization problem.

Position of the source is related to some metric of measurement. These measurements are fall into several categories, in which the localization solutions are based on different types of physical measures: Time of Arrival (TOA) [1], [2], Time Difference of Arrival (TDOA) [3]–[6], Direction of Arrival (DOA) [7]–[9]; and Received Signal Strength (RSS) or Energy [10], [11].

Many works have transferred these physical measurements to distances between source and anchors. Then the input of localization will be a distance matrix, for example, [12], [13]. Compared with the TDOA and the DOA methods, RSS- or Energy-based approaches are attractive because they are widely applicable. They do not require additional hardware and can reuse the existing wireless infrastructure. The RSS of a signal traveling between two transceivers is a signal parameter that contains information related to the distance between them. This RSS information can be used in conjugation with a suitable attenuation model and shadowing effect to estimate distance. The shadowing effect is commonly modeled as a zero-mean Gaussian random variable with a variance of in the logarithmic scale.

In a centralized algorithm, the source transmits the data to a central point or a fusion center. Then the ultimate goal is to estimate the source location based on the RSS samples and known anchor locations. Source localization techniques using RSS measurements can be divided into four categories: maximum likelihood (ML), LS-based, Semidefinite programming (SDP) based, and second-order cone programming (SOCP) based. The ML and LS-based methods are highly nonconvex, so finding the global optimum is often with high computational complexity, especially for a large-scale problem.

For the same reason, a good initial point is vital to avoid local minima as possible. SDP based and SOCP based methods deal with the non-convexity problem by relaxing the non-convex constraints in original problems so that they can be transferred into convex ones. For these methods, the tightness of the relaxation shall be considered to guarantee accuracy. And it is shown that though SOCP relaxation has a more straightforward structure and can be solved faster, it is weaker than SDP method [14].

In reality, anchor's position information may have errors though some research works neglect it. Inaccurate anchors

will deteriorate the localization performance. So in recent years, there has been an increasing interest in determining the position of the source in the presence of inaccurate position of anchors [15]–[20]. [20] proposed a min-max method for the relative location estimation problem by minimizing the worst-case estimation error. And this work uses SDP technique to relax the original nonconvex problem into a convex one. [16] focused on differential received signal strength (DRSS)-based localization with model uncertainties such as unknown transmit power, PLE, and anchor location errors. [18] performs analysis and develops a solution for locating a moving source using time-difference-of-arrival (TDOA) and frequency-difference-of-arrival (FDOA) measurements in the presence of random errors in anchor locations. [15] devised a convex relaxation leading to a SOCP. It proposed a mixed robust SDP-SOCP framework to benefit from the better accuracy of SDP and the lower complexity of SOCP. [17] uses TDOA information, considered the sensor node's (anchor) bounded location error effect.

Lohrasbipeydeh et.al. [21] factor the MSE into two independent terms corresponding to the geometric distribution of the sensors and the channel parameters, including the noise variance. Then derive the effect of the sensor and source location to the localization accuracy. This study uses a geometric dilution of precision to calculate the MSE. This study also uses the same method to evaluate the effect of the joint estimation of unknown power and source location on the performance.

Yongchang et al. [16] focus on differential received signal strength (DRSS)-based localization with model uncertainties in case of unknown transmit power and PLE. This study presents a robust SDP-based estimator (RSDPE), which can cope with imperfect PLE and inaccurate anchor location information.

Xiaoping et.al. [22] proposes a cooperative motion parameter estimation method using RSS measurement to estimate target motion parameters cooperatively. At first, this study uses a nonconvex model to determine the initial positions and velocity. Then use an unconstrained SDP model to estimate the positions of the mobile targets. This study assumes the transmit powers to be known.

III. ROBUST LOCALIZATION CONSIDERING INEXACT ANCHORS

A. Problem Model Formulation

After successful demodulation, RSS refers to the signal power. RSS can be computed from the demodulated signal envelope $r(t) = x(t) \oplus h(t)$. Here \oplus denotes the convolution operator, $x(t)$ is the transmitted signal, $h(t)$ denotes the wireless channel response. Collecting RSS measurements from a demodulated signal in a real environment can be easy to implement utilizing given hardware.

The received signal envelope is always modeled using specific probability distribution function such as Rician, Rayleigh, Log-normal, or Nakagami-m [23].

Remove the time index t , let r denotes the envelope of instantaneous received signal power. And let Ω denotes the RSS

to be collected. Considering the distribution of r described above, apparently, the maximum likelihood estimate of Ω is

$$\hat{\Omega} = \frac{1}{K} \sum_{k=1}^K r^{(k)} \quad (1)$$

Eq.(1) is unbiased and it means the RSS of the i -th anchor can be computed by collecting K consecutive samples of r . This is easy to accomplish and does not require additional hardware for any wireless receiver.

The signal strength measurement is subject to a complicated radio propagation channel. In this paper, the log-normal shadowing model is used to characterize the RSS. The RSS(from the source and received by the i -th anchors), which is denoted as Ω_i , can be related to the distance between the source and the i -th anchor through the path loss model for wireless transmission [23].

$$L_i = L_0 + 10\gamma \log_{10} \frac{\|x - z_i\|}{d_0} + n_i \quad (2)$$

Where $L_i = P_T - \Omega_i$ is the path loss, and P_T is assumed to be known. Here n_i is a Gaussian random variable representing the log-normal shadow fading effect in multi-path environments. L_0 denotes the path loss value at the reference distance d_0 . γ indicates the path loss exponent.

Suppose that there are M location-aware anchors and one location-unaware source. For $i = 1, 2, \dots, M$, let $z_i \in R^2$ denotes the true positions of the anchors. In practice, the known position of anchors are corrupted with location errors. The relationship between the true position z_i and the inexact position \hat{z}_i can be defined by

$$z_i = \hat{z}_i + \Delta_i, \quad \text{for } i = 1, 2, \dots, M \quad (3)$$

where the error here assumed bounded, so

$$\|\Delta_i\| \leq \zeta \quad (4)$$

in (4), $\|\cdot\|$ denotes the Euclidean norm. Here it is not needed to specify the distribution precisely of the error.

It is easy to derive from (2) that the corresponding Maximal Likelihood estimator is

$$x_P = \arg \min_x \sum_{i=1}^M \left(10\gamma \log_{10} \frac{\|x - z_i\|}{d_0} - (L_i - L_0) \right)^2 \quad (5)$$

Let

$$\beta_i^2 = d_0^2 10^{\frac{L_i - L_0}{5\gamma}} \quad (6)$$

Then, the ML estimator (5) can be transformed into

$$x_P = \arg \min_x \sum_{i=1}^M \left(\log_{10} \frac{\|x - z_i\|^2}{\beta_i^2} \right)^2 \quad (7)$$

Considering Eq.(3), an optimization approach is proposed for the location estimation of the source in the following:

$$x_P = \arg \min_x \sum_{i=1}^M \left(\log_{10} \frac{\|x - z_i\|^2}{\beta_i^2} \right)^2 \quad (8)$$

s.t. $z_i = \hat{z}_i + \Delta_i$

For worst-case design, considering Eq.(4), we can modify (8) as a min-max optimization problem:

$$x_P = \arg \min_x \max_{\|\Delta_i\| \leq \zeta} \sum_{i=1}^M \left(\log_{10} \frac{\|x - z_i\|^2}{\beta_i^2} \right)^2 \quad (9)$$

s.t. $z_i = \hat{z}_i + \Delta_i$

By applying the Taylor expansion, the term $\|x - z_i\|$ in Eq.(9) can be expanded as

$$\|x - z_i\| = \|x - \hat{z}_i\| - \frac{\Delta_i^T (x - \hat{z}_i)}{\|x - \hat{z}_i\|} + o(\|\Delta_i\|) \quad (10)$$

Let $\delta_i = \frac{\Delta_i^T (x - \hat{z}_i)}{\|x - \hat{z}_i\|}$, then

$$|\delta_i| \leq \zeta \quad (11)$$

Using (10) and (11), Eq.(9) can be transformed into

$$x_P = \arg \min_x \max_{|\delta_i| \leq \zeta} \sum_{i=1}^M \left(\log_{10} \frac{(\|x - \hat{z}_i\| - \delta_i)^2}{\beta_i^2} \right)^2 \quad (12)$$

which can also be written as

$$x_P = \arg \min_x \max_{|\delta_i| \leq \zeta} \left| \log_{10} \frac{(\|x - \hat{z}_i\| - \delta_i)^2}{\beta_i^2} \right|^2 \quad (13)$$

B. The Relaxation Procedure

Obviously, problem (13) is not convex. One can see that $\{x : \|x - \hat{z}_i\| = \delta_i\}$ is not in the objective function domain. And the source can not overlap with the anchors, so each anchor is also a singular point. It is difficult to find and confirm the global minimum solution.

To obtain a convex formulation so that the existing numerical algorithms can be employed, the problem is transformed and relaxed, as shown in the following steps.

Using Chebychev approximation, i.e., this paper use l_∞ -norm to replace $\|\cdot\|^2$ in (13), then get

$$x_P = \arg \min_x \max_i \left| \log_{10} \frac{(\|x - \hat{z}_i\| - \delta_i)^2}{\beta_i^2} \right| \quad (14)$$

s.t. $|\delta_i| \leq \zeta$

Noting that

$$\begin{aligned} & \left| \log_{10} \frac{(\|x - \hat{z}_i\| - \delta_i)^2}{\beta_i^2} \right| \\ &= \max \left(\log_{10} \frac{(\|x - \hat{z}_i\| - \delta_i)^2}{\beta_i^2}, \log_{10} \frac{\beta_i^2}{(\|x - \hat{z}_i\| - \delta_i)^2} \right) \end{aligned} \quad (15)$$

Since $\log_{10}(x)$ is a strictly monotonically increasing function in its domain $(0, +\infty)$, Eq.(14) can be transformed into

$$\begin{aligned}
x_P &= \arg \min_x \max_i (\log_{10} \frac{(\|x - \hat{z}_i\| + \zeta)^2}{\beta_i^2}, \\
&\quad \log_{10} \frac{\beta_i^2}{(\|x - \hat{z}_i\| - \zeta)^2}) \\
&= \arg \min_x \max_i \log_{10} \left(\frac{(\|x - \hat{z}_i\| + \zeta)^2}{\beta_i^2}, \frac{\beta_i^2}{(\|x - \hat{z}_i\| - \zeta)^2} \right) \\
&= \arg \min_x \max_i \left(\frac{(\|x - \hat{z}_i\| + \zeta)^2}{\beta_i^2}, \frac{\beta_i^2}{(\|x - \hat{z}_i\| - \zeta)^2} \right)
\end{aligned} \tag{16}$$

Here we assume that $\|x - \hat{z}_i\| - \zeta > 0$, this is reasonable since the inaccuracy of anchor's position is relatively small compared to the distance between source and anchors. Considering the "worst-case" situation, just substitute δ_i to ζ . Noticing that (16) is still not convex. Introducing an auxiliary variable $k \in \mathbb{R}^+$. Then Eq.(16) can be transformed into

$$\begin{aligned}
x_P &= \arg \min_{x,k} k \\
s.t. \quad &\frac{(\|x - \hat{z}_i\| + \zeta)^2}{\beta_i^2} \leq k \quad i = 1, \dots, M \\
s.t. \quad &\frac{\beta_i^2}{(\|x - \hat{z}_i\| - \zeta)^2} \leq k \quad i = 1, \dots, M
\end{aligned} \tag{17}$$

Noting that

$$\begin{aligned}
(\|x - \hat{z}_i\| + \zeta)^2 &= \|x - \hat{z}_i\|^2 + 2\zeta\|x - \hat{z}_i\| + \zeta^2 \\
(\|x - \hat{z}_i\| - \zeta)^2 &= \|x - \hat{z}_i\|^2 - 2\zeta\|x - \hat{z}_i\| + \zeta^2
\end{aligned} \tag{18}$$

and

$$\|x - \hat{z}_i\|^2 = x^T x - 2x^T \hat{z}_i + \hat{z}_i^T \hat{z}_i \tag{19}$$

Let $X = xx^T \in \mathbb{S}^2$, then (19) can be cast as

$$\|x - \hat{z}_i\|^2 = \text{tr}(X) - 2x^T \hat{z}_i + \hat{z}_i^T \hat{z}_i \tag{20}$$

Where $\text{tr}(X)$ denotes the trace of the auxiliary variable $X \in \mathbb{S}^2$.

Introducing auxiliary variable $l \in \mathbb{R}^{M \times 1}$, where $l_i = \|x - \hat{z}_i\|$, $i = 1, \dots, M$, Letting $L = ll^T$, then

$$L(i, i) = \text{tr}(X) - 2x^T \hat{z}_i + \hat{z}_i^T \hat{z}_i \tag{21}$$

Apparently, we have

$$L(i, j) \geq 0 \tag{22}$$

Incorporating (18) (20) (21) (22) into (17), a formulation modified from (17) is obtained as

$$\begin{aligned}
x_P &= \arg \min_{x,k,l,X,L} k \\
s.t. \quad &\text{tr}(X) + 2x^T \hat{z}_i + \hat{z}_i^T \hat{z}_i + 2\zeta l_i + \zeta^2 \leq k\beta_i^2 \\
&\text{tr}(X) + 2x^T \hat{z}_i + \hat{z}_i^T \hat{z}_i - 2\zeta l_i + \zeta^2 \geq k^{-1}\beta_i^2 \\
&L(i, i) = \text{tr}(X) - 2x^T \hat{z}_i + \hat{z}_i^T \hat{z}_i \\
&L(i, j) \geq 0 \\
&X = xx^T \\
&L = ll^T \\
&k \geq 0 \\
&i, j = 1, \dots, M
\end{aligned} \tag{23}$$

In (23), $\text{tr}(X) + 2x^T \hat{z}_i + \hat{z}_i^T \hat{z}_i + 2\zeta l_i + \zeta^2 \leq k\beta_i^2$ are affine constraints. $\text{tr}(X) + 2x^T \hat{z}_i + \hat{z}_i^T \hat{z}_i - 2\zeta l_i + \zeta^2 \geq k^{-1}\beta_i^2$ are convex constraints since $\text{tr}(X)$ is linear in X , $x^T \hat{z}_i$ is linear in x and k^{-1} is convex in k . $X = xx^T$ and $L = ll^T$ mean that X and L are rank one symmetric positive semidefinite (PSD) matrix, which means that $X \succeq 0$, $\text{rank}(X) = 1$ and $L \succeq 0$, $\text{rank}(L) = 1$. It can be noticed that the fundamental difficulty in solving Eq.(23) are the rank one constraints, which is nonconvex (the set of rank one matrices is not a convex set), the objective function and all other constraints are convex in x, k, l, X, L . Thus we may as well drop it to obtain the relaxed version of (23). That means, using Schur complement,

$$\begin{aligned}
X \succeq xx^T &\Rightarrow \begin{pmatrix} X & x \\ x^T & 1 \end{pmatrix} \succeq 0 \\
L \succeq ll^T &\Rightarrow \begin{pmatrix} L & l \\ l^T & 1 \end{pmatrix} \succeq 0
\end{aligned} \tag{24}$$

At the same time, using Schur complement, the paper expresses $\text{tr}(X) + 2x^T \hat{z}_i + \hat{z}_i^T \hat{z}_i - 2\zeta l_i + \zeta^2 \geq k^{-1}\beta_i^2$ as follows LMI form:

$$\begin{pmatrix} \text{tr}(X) + 2x^T \hat{z}_i + \hat{z}_i^T \hat{z}_i - 2\zeta l_i + \zeta^2 & \beta_i \\ \beta_i & k \end{pmatrix} \succeq 0 \tag{25}$$

$i = 1, \dots, M$

Combining (24), (25) with (23), the received signal strength based robust location estimation for the target problem is as follows:

$$\begin{aligned}
x_P &= \arg \min_{x,k,l,X,L} k \\
s.t. \quad &\text{tr}(X) + 2x^T \hat{z}_i + \hat{z}_i^T \hat{z}_i + 2\zeta l_i + \zeta^2 \leq k\beta_i^2 \\
&\begin{pmatrix} \text{tr}(X) + 2x^T \hat{z}_i + \hat{z}_i^T \hat{z}_i - 2\zeta l_i + \zeta^2 & \beta_i \\ \beta_i & k \end{pmatrix} \succeq 0 \\
&L(i, i) = \text{tr}(X) - 2x^T \hat{z}_i + \hat{z}_i^T \hat{z}_i \\
&L(i, j) \geq 0 \\
&\begin{pmatrix} X & x \\ x^T & 1 \end{pmatrix} \succeq 0 \\
&\begin{pmatrix} L & l \\ l^T & 1 \end{pmatrix} \succeq 0 \\
&k \geq 0 \\
&i, j = 1, \dots, M
\end{aligned} \tag{26}$$

In Eq.(26), $x \in \mathbb{R}^2$ represents the position of interest. x_P represents the corresponding estimator of the decision variable x . The remaining variables are $k \in \mathbb{R}$, $l \in \mathbb{R}^M$, $X \in \mathbb{R}^{M \times M}$, $L \in \mathbb{R}^{M \times M}$. All constraints in Eq.(26) are expressed by matrix inequalities. Eq.(26) is an instance of semidefinite programming (SDP) and also a relaxation of Eq.(17). Eq.(26) can be solved, to any arbitrary accuracy, in a numerically reliable and efficient fashion.

C. Rounding the Solution

When using the aforementioned relax techniques, further modification is always needed. The word 'modification' contains two meanings. At first, converting a globally optimal solution x_P of problem Eq.(26) into a feasible solution \tilde{x} to problem Eq.(23). Furthermore, from the solution of Eq.(26), the rounding procedure can generate a series of candidates 'nearby' and select the 'best match' of the original problem's constraints.

An intuitively appealing idea is to apply the rank-one approximation on the solution X^* , L^* , x and l of Eq.(26). This approach uses the largest eigenvalue λ_{xM} and the corresponding eigenvector q_{xM} to approximate X^* , use λ_{lM} and corresponding eigenvector q_{lM} to approximate L^* . Then if $\sqrt{\lambda_{xM}}q_{xM}$ and $\sqrt{\lambda_{lM}}q_{lM}$ are feasible to Eq.(23), the solution \tilde{x} is got. Otherwise $\sqrt{\lambda_{xM}}q_{xM}$ and $\sqrt{\lambda_{lM}}q_{lM}$ need to be mapped to nearby feasible solution in a problem dependent way.

Randomization is another way to extract an approximate solution from an SDR solution. The intuitive idea of this method is to use $X - xx^T$ of Eq.(26) as a covariance matrix. This study generates random vectors $\xi_x \sim N(0, X)$, then use the random vector to construct an approximate solution in a problem-dependent way. The rounding procedure using randomization is described in Alg.1.

In Alg.1, to generate $\xi_x(t)$, we simply generate a random vector u whose components are i.i.d $N(0, 1)$, then let $\xi_x(t) = V^T u + x^o$, where V is the factorization matrix $X^* - x^o x^{oT} = V^T V$. And since $X^* - x^o x^{oT} \geq 0$, so that V always existed. In, Alg.1, the procedure Alg.2 is called to create a feasible solution of Eq.(23).

Other than the randomization method, an alternative strategy to search the feasible solution x utilizing the information given by SDR is through grid search. This method may reduce the searching space significantly compared with randomization method, at the same time, keep the accuracy. It is logical because for a Gaussian random vector $\xi_x(t)$ generated in Alg.1 will exist close to the mean with a high probability. Then the randomization method will waste some trials in the 'sparse' area. It is also reasonable to adapt the variable step size algorithm to improve the grid searching performance and balance the computation complexity. In this paper, an adaptive variable step size based grid searching rounding algorithm is proposed in Alg.3. Note that in Alg.3 a mechanism is designed to reduce the searching space when the candidate point x^o is far from the mean x^* . And Alg.3 restrict the searching scope to $3 * \max([X^*]_{1,1}, [X^*]_{2,2})$. Considering the one-dimensional situation, given a Gaussian random variable x , then $P(\|x - E(x)\| \leq 3\sigma_x) \geq 0.999$. That means the

searching scope is large enough to find the best candidate point.

It is convenient and straightforward that refine the estimation by using the solution of Eq.(26) as an initial point for the original problem Eq.(2) and run a local optimization method. However, the original problem Eq.(2) is non-differentiable and not very smooth. Eq.(23) is smooth and asymptotic optimal. But this problem's constraint is complicated and so that it is challenging to compute the Newton step when dealing with not feasible initial points and iterates.

In this study, however, all rounding methods introduced above are based on the inaccurate anchor position information. This weakness limits the higher rounding performances relating to the final localization accuracy. This paper proposes a new rounding approach named 'r-r' (Rounding Original Problem). Tr-r considers both of the two types of errors. One is between the approximation x^* get from Eq.(26) and the real source location. Another is between the real anchor position and the inaccurate anchor position. Because the power loss $L(i)$ in each anchor is reliable based on the real anchor and source position. This paper uses the $L(i)$ information to calculate the best matching of the potential source location and real potential anchors simultaneously. Fig.1 illustrate the basic idea of r-r. In this figure, near every given anchor position (inaccurate), r-r generates several possible real anchor candidate positions (denotes by the left-pointing triangle) within the range of ζ . At the same time, r-r generates several possible position candidate of the source near the solution x . This step is just the same as described in Alg.1. Next, from anchor candidate group of each inaccurate anchor, r-r selects one anchor candidate, and so that form an anchor candidate position vector. And the r-r rounding algorithm is described in Alg.4 in detail.

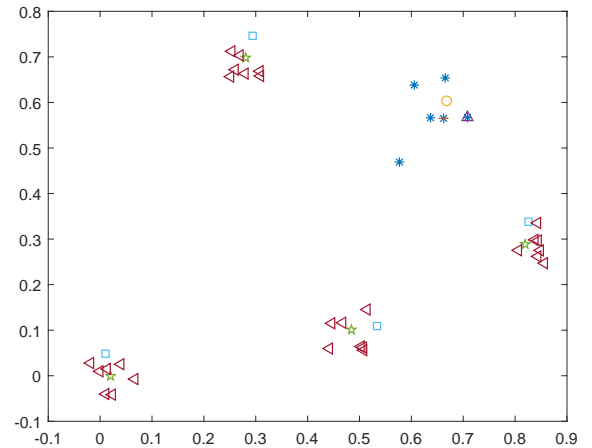


Fig. 1. Illustration of the r-r rounding method. The circle denotes the real source location. Plus sign denotes the solution get from Eq.(26). The asterisk denotes the generated random source location. Square denotes the accurate anchor position. Pentagram denotes the in-accurate anchor position. Left-pointing triangle denotes the generated random anchor candidates position. Upward-pointing triangle denotes the final rounding result. Note that in this figure, the Upward-pointing triangle does not certainly represent the asterisk closest to the circle. This phenomenon is reasonable because the r-r method (actually, all rounding methods) only works on average.

Note that all rounding strategies described above can only be applied to SDP relaxation. Other types of relaxation (e.g., SOCP) of Eq.(23) may not use these rounding methods directly. That is because there is no information about the variance matrix to guide the random solution generating procedure. Random generation of feasible points will lead the rounding process impossible to compute.

Algorithm 1 Refine By Randomization

Require: x^*, X^*, tt \triangleright tt is the number of randomization
Ensure: x
 1: $x^o \leftarrow x^*$
 2: **for** $t = 1 : tt$ **do**
 3: Generate random vector $\xi_x(t) \sim N(x^o, X^* - x^o x^{oT})$
 4: $k_o(t) \leftarrow \text{ComputeK}(\xi(t), M)$
 5: $t \leftarrow \arg \min_t k_o(t)$
 6: $x \leftarrow \xi_x(t)$

Algorithm 2 Create Feasible Solution

1: **procedure** COMPUTEK(ξ, M) \triangleright Number of anchors
 2: $X^o \leftarrow \xi_x \xi_x^T$
 3: **for** $i=1:M$ **do** $l_i^o \leftarrow \|x^o - \hat{z}_i\|$
 4: $L^o \leftarrow [l_i^o]_{i=1:M}$
 5: Compute k^o using X^o, L^o, ξ, l^o in Eq.(23)

Algorithm 3 Refine By Variabe Step Grid Searching

Require: x^*, X^*
Ensure: x
 1: $x^o \leftarrow x^*$
 2: $\sigma_d \leftarrow \max([X^*]_{1,1}, [X^*]_{2,2})$
 3: $d_s \leftarrow 0.0001$
 4: $\Delta_{d_s} \leftarrow 0.001 * \sigma_d$
 5: **while** $d_s = \|x^o - x^*\| \leq 3\sigma_d$ **do**
 6: $\iota = \text{fix}(\frac{1}{d_s})$
 7: $[\Delta_x]_{1..\iota} \leftarrow [d_s * \cos(2\pi * \frac{1..\iota}{\iota})]$
 8: $[\Delta_y]_{1..\iota} \leftarrow [d_s * \sin(2\pi * \frac{1..\iota}{\iota})]$
 9: $[\xi]_{1..\iota} \leftarrow x^o + [\Delta_x, \Delta_y]^T$
 10: $k_o \leftarrow \text{ComputeK}(\xi, M)$
 11: $d_s \leftarrow d_s + \Delta_{d_s}$
 12: $t \leftarrow \arg \min_t k_o(t)$
 13: $x \leftarrow \xi_x(t)$

IV. SIMULATION RESULTS AND ANALYSIS

In this section, we discuss the performance evaluation of numerical results based on MATLAB. This paper conducts Monte Carlo simulation to average out the effect of the geometric layout and random noise and error. For each MC trial, every anchor location is given with a casual but bounded deviation. This paper uses the Root Mean Square Error(RMSE) as the performance criterion. That is, smaller RMSE indicates better localization performance. Different localization methods are performed to calculate the RMSE in the same scenario for comparison.

Algorithm 4 Refine considering Inaccurate Anchors

Require: $x^*, X^*, tt, \zeta, \hat{z}, \text{nac}$ \triangleright nac is the number of random anchor candidates
Ensure: x
 1: $x^o \leftarrow x^*$
 2: **for** $t = 1 : tt$ **do**
 3: Generate random vector $\xi_x(t) \sim N(x^o, X^* - x^o x^{oT})$
 4: **for** $i = 1 : \text{nac}$ **do**
 5: Generate random vector $n_i \in R^{2 \times 1}, \|n_i\| \leq \zeta$
 6: Generate random vector $\text{pr}_i = \hat{z}_i + n_i$
 7: $\text{sit} \in R^{2 \times \text{size}(\hat{z}, 2) \times \text{nac}} \leftarrow$ Permutation of pr_i
 8: Compute Vector $|x - \text{sit}(:, :, 1 : \text{nac})|$
 9: $x \leftarrow \arg \min_x |x - \text{sit}|$

We use different scenarios, and parallels each random walk by MATLAB command "parfor-loop". We expect that additional code optimization and C implementation can further reduce the CPU time needed. The optimum number of Monte Carlo trials is derived in Appendix A.

We use CVX [24] for specifying the convex problem, with SDPT3 [25] as solver. Note that currently CVX can not be used in the parallel loop. We circumvented this problem by defining a function that contains the CVX code then call it in the 'parfor' loop.

We use modified ML estimation('ml') [26], SDP-RSS('rss') [27], SDP-DISTANCE('p-d') using pairwise distance information [20], SOCP-RSS('so') modified from [6] using RSS and SOCP-DISTANCE('so-d') using pairwise distance information modified from [14] to compare with our proposed Robust-RSS('ro') method. All distance based methods assumes that the distance information is get through TOA. Considering multi-path and NLOS transmission effect, the distance error variance introduced is set to 0.15 [28]. SOCP-RSS method is relaxed from(17) , (18) as:

$$\begin{aligned}
 x_P &= \arg \min_{x,k} k \\
 s.t. \\
 \|x - \hat{z}_i\| &\leq \frac{1}{\zeta} (k\beta_i^2 - \zeta^2) \\
 \|x - \hat{z}_i\|^2 + \zeta^2 &\geq k^{-1}\beta_i^2, \dots, M \\
 i &= 1, \dots, M
 \end{aligned} \tag{27}$$

consider that $\|x - z_i\| \gg \zeta$, Eq.(27) can be transferred into

$$\begin{aligned}
 x_P &= \arg \min_{x,k} k \\
 s.t. \\
 \|x - \hat{z}_i\| &\leq \frac{1}{\zeta} (k\beta_i^2 - \zeta^2) \\
 \begin{pmatrix} k & \beta_i \\ \beta_i & \|x - \hat{z}_i\| \end{pmatrix} &\succeq 0 \\
 i &= 1, \dots, M
 \end{aligned} \tag{28}$$

then Eq.(28) can be transformed into

$$\begin{aligned}
x_P &= \arg \min_{x,k,t} k \\
s.t. \\
\|x - \hat{z}_i\| &\leq \frac{1}{\zeta}(k\beta_i^2 - \zeta^2) \\
\begin{pmatrix} k & \beta_i \\ \beta_i & t(i) \end{pmatrix} &\succeq 0 \\
\|x - \hat{z}_i\| &\leq t(i) \\
i &= 1, \dots, M
\end{aligned} \tag{29}$$

Clearly Eq.(29) is a Second-Order Cone Programming problem and can be solved by existing numerical methods efficiently. SOCP-DISTANCE is obtained as

$$\begin{aligned}
x_P &= \arg \min_{x,k,t} k \\
s.t. \\
t(i) - \beta(i)^2 &\leq k \\
t(i) - \beta(i)^2 &\geq -k \\
t(i) &\geq 0 \\
i &= 1, \dots, M
\end{aligned} \tag{30}$$

The modified ML-RSS estimator (5) is solved using MATLAB function 'lsqnonlin'.

For the simulations, anchors and the source are located in a 1×1 rectangle area. For simplicity, the communication range in each topology is not concerned. We apply a fixed link error model with equal noise variances for σ^2 for all links, i.e., a link with a long distance does not have a larger noise for simplicity. We set $d_0 = 0.025$, $L_0 = 8$, $\gamma = 3$ [23]. Note that in this study, we do not care about the absolute distance. The relative distance is adopted because the SDPT3 solver needs numerically easy input. If the elements of the problem are somewhat large in magnitude, that may cause numerical non-goodness. In this situation, a scaling procedure is necessary.

In order to explain the phenomena, for example, if the length of side of the deploy region is set to 400m (or some number in an actual deployment scenario), then reported (sort of) optimal X in Eq.(26) may has elements in the $1e4$ or $1e5$ magnitude, which is causing numerical non-goodness. Because the elements in X^* are large, the minimum eigenvalue of $X - xx^T$ has a significantly different magnitude than that of $\begin{pmatrix} X & x \\ x^T & 1 \end{pmatrix}$. So a very small magnitude negative min eigenvalue of $\begin{pmatrix} X & x \\ x^T & 1 \end{pmatrix}$ can, and in this case does, correspond to a much larger magnitude negative min eigenvalue of $X - xx^T$. The solver only knows the constraint $\begin{pmatrix} X & x \\ x^T & 1 \end{pmatrix} \succeq 0$, and therefore works to satisfy that within tolerance (but maybe does not achieve that with Eq.(26)). So then the "violation" in terms of the minimum eigenvalue of $X - xx^T$ can be much large, and SDPT3 solver will fail to give a feasible solution. The simulation should strive to get the non-zero elements of the optimal X^* to be much closer to one in magnitude. This paper does not try to scale the input, just using the relative

distance is a good and simple choice to avoid the numerical non-goodness. Using commercial solvers such as CPLEX [29] may improve by completing the scaling process automatically, but in this paper, we do not test.

In wireless localization problems, the impact of anchor node placement always should be considered. Of course, the geometric layout of anchors and the target has a significant impact on the localization accuracy for the "convex hull" effect of anchors [30]–[32]. It is also easy to imagine that if anchors are deployed close to each other, then the localization problem will be ill-conditioned so that it is more sensitive to the inaccuracy and noise. As shown in Fig.2, two types of simulation are conducted, one with 'good' anchor placement, the other is with 'bad' anchor placement. This paper does not investigate the optimal geometric layout. Some related works are proposed in [33].

This study calculates Cramer-Rao lower bound(CRLB) in Appendix B as a benchmark. The CRLB represents the minimum RMSE that any unbiased location estimator can achieve theoretically.

A. Impact of Anchor Location Error Level

Fig. 3 shows the average localization RMSE, computed by averaging for all the scenarios which have the same σ and M , as a function of ζ with three anchors. The noise variance parameter is set to zero. As can be seen, all estimators behave worse with an increasing error bound of the anchor location inaccuracy, but 'ro' method plus proposed rounding algorithm considering inaccurate anchor position('r-r') yields the best performance, due to its design for coping with model uncertainties. As shown in Fig.3a, when the anchors are absolutely random deployed, then ml and rss methods are entirely ineffective overall error level. As a contrast, Fig.3b shows if the anchors are designed placed and the source always falls into the convex hull of anchors, then the so-p method can give a lower quality result. As can be seen in both Fig.3a and Fig.3b, the proposed ro, and r-r methods are much slower and steadier compared with p-d and so methods. From Fig.3a, there is a significant positive correlation between performance improvement and ro together with r-r rounding method when the location error level ζ is high ($\zeta = 0.16$). However, in Fig.3b, the improvement is not obvious because the performance before rounding is good enough due to the convex hull effects. It is worth noting that even in Fig.3b, where the localization accuracy is relatively high, the improvement of ro and r-r methods are significant compared with so and p-d estimators. In high error situation($\zeta = 0.16$), there is also approximate 30% accuracy improvement. One other important note, the error level ζ is the worst error bound, and hence, the proposed method is a worst-case design.

Fig.6 is the boxplot of RMSE for the different level of anchor errors. The more robust estimator in the boxplot will have a shorter length(narrower error distribution) and lower median mark. For brevity, 'r-p' rounding methods is omitted since its error distribution is very similar to 'r-g'. As shown in Fig.6, the proposed ro, and r-r methods have superior performance in terms of lower value of RMSE and narrower

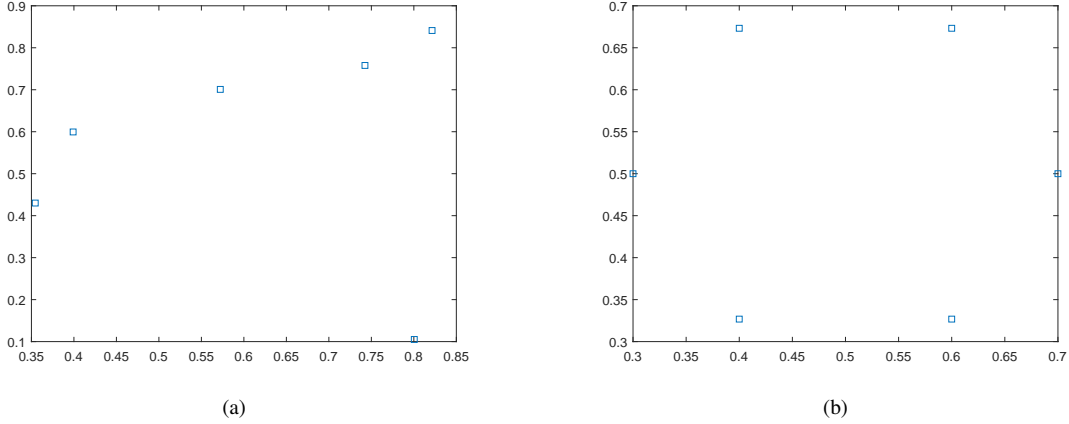


Fig. 2. Two types of anchor placement. in (a), anchors are randomly placed. In (b) anchors are placed by design. It is obvious that a target will reside within the convex hull of anchors with a high probability.

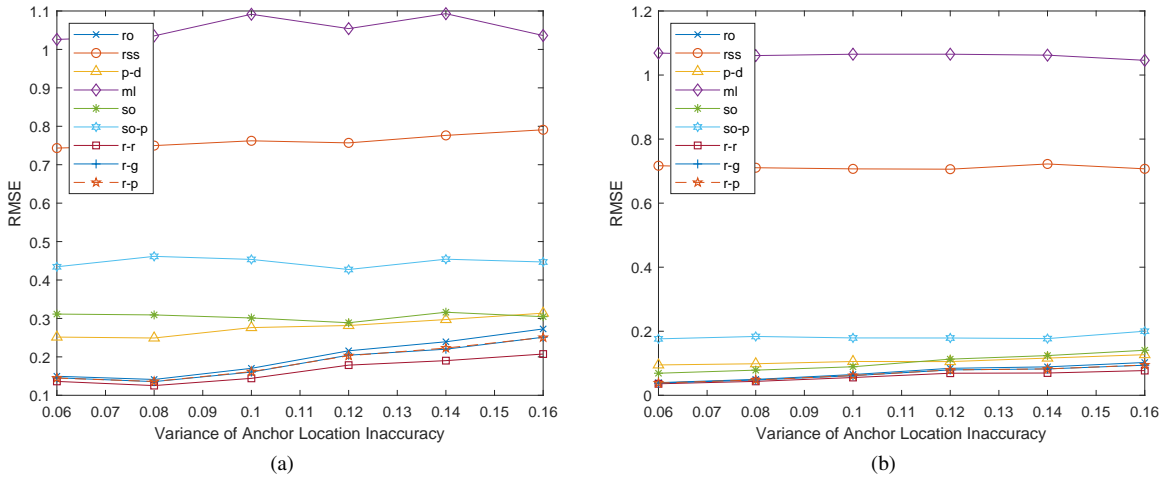


Fig. 3. Numerical simulation results of different methods with various value of anchor location error ζ . $\sigma = 0$, number of anchors $M = 3$. (a) is "RMSE Versus ζ " plot under 'bad' anchor placement as shown in Fig.2a. (b) is under 'good' anchor placement as shown in Fig.2b. 'ro' denotes the robust localization algorithm. 'rss' denotes SDP-RSS [27]. 'p-d' denotes SDP-DISTANCE using pairwise distance information [20]. 'ml' denotes modified ML estimation [26]. 'so' denotes SOCP-RSS modified from [6] using RSS,'so-d' denotes SOCP-DISTANCE using pairwise distance information modified from [14]. 'r-r' denotes the proposed robust localization algorithm using rounding method Alg.4.

distribution. The distribution of 'M' is the widest among all the localization methods. Since the performance of 'M' estimator depends heavily on the starting point, this method is impractical. The other thing to note in Fig.6 is that there are very fewer data points beyond the box in Fig.6b compared within Fig.6a. This phenomenon indicates another advantage of the convex hull effect.

B. Impact of Measurement Noise Level

The RSS measurement noise includes the shadowing effect and transmits power derivations. The effect of the standard deviation of the log-normal shadow fading variable on localization accuracy has been shown in Fig.4. We study all localization methods under large and small measurement noise with $\zeta = 0.06$ and $M = 3$ averaged in uniformly-random network topologies. Fig.4a is under totally random anchor placement, while Fig.4b is under 'good' anchor placement. The following observations can be made: No matter the anchor deployment, the performance of any methods shows degradation as the noise standard deviation increases. ro and

r-r outperform all other methods. SDP-based methods perform better than SOCP-based methods due to the tighter relaxation on the problem. Measurement noise does not influence the localization performance significantly compared with anchor location error. It should be noted that RSS measurement noise is unrelated to distance-based methods. This is because that distance information in this study is assumed getting from TOA.

C. Impact of Number of Anchors

In addition to anchor location inaccuracy and measurement noise, the number of anchors also impacts the performance. In the simulations, we vary the number of anchors from 3 to 6 while keeping the anchor location inside the square deployment region. For each number of anchors, a similar procedure as has been described above is done to calculate the average RMSE.

Fig.8 shows the average RMSEs versus different numbers of anchors with two types of anchor deployments. As expected, the estimation error will generally be reduced if the number

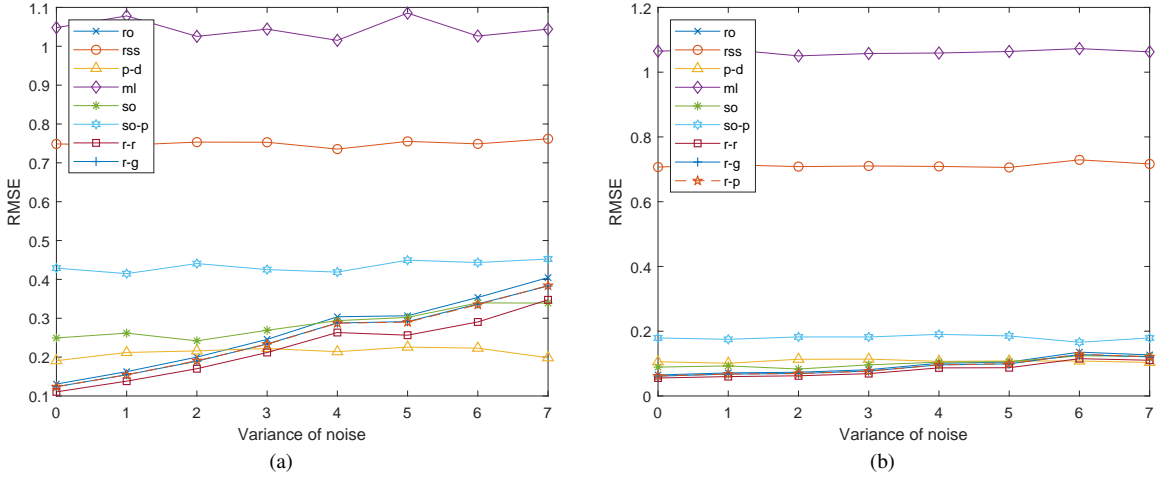


Fig. 4. Numerical simulation results of different methods with various value of noise σ ($\zeta = 0.06$, number of anchors $M = 3$). (a) is "RMSE Versus σ " plot under 'bad' anchor placement as shown in Fig.2a. (b) is under 'good' anchor placement as show in Fig.2b.

of anchors is increased in random anchor deployments. Fig.5a show this phenomena. As shown in Fig.5b, because the RMSE is fairly low in good anchor placement, so the effects of anchor number are not as apparent as in Fig.5a.

As can be observed in both Fig.5a and Fig.5b, ro and r-r achieves the high accuracy. For Fig.5a, the possible probability of the estimation locations lying in the convex hull of the anchors increase if the number of anchors becomes greater so that when the anchor number is changed from 3 to 5, the performance improved significantly for ro,r-r,p-d, and so-p. Fig.8 is the boxplot of RMSE of different methods corresponding with different anchor numbers. As shown in Fig.8, when the number of anchors increases, the width of the RMSE distribution for ro,r-r reduce, and the median mark corresponding with ro and r-r also decline.

V. CONCLUSION AND FUTURE WORKS

This paper set out to address the source localization problem using RSS measurement. The anchors used for localization are with inaccurate location information. The RMSE is used as the performance indicator of the proposed method.

This paper proposes a relaxed convex SDP estimator. This estimator considers the worst case possible error of location for all anchors. To further improve the performance, this paper studies different kind of rounding methods and proposes a rounding algorithm considering both the anchor location error and the source location error.

Simulations have evidenced that the proposed method outperforms the selected existing methods, and complied well with the RSS measurement model. Rather than focusing on some particular topologies of anchor placement, the random deployment of anchors has been considered. The influence of different environmental parameters on the localization performance has been examined. The proposed method does not need a good starting point for the solving process and a proper deployment of anchors.

A further study should expand the framework established in this paper to other practical scenarios, such as wireless sensor

networks localization. Further research should also be undertaken to consider the self-estimation of wireless propagation parameters in the estimator formulation.

APPENDIX A OPTIMAL NUMBER OF TRIALS FOR MONTE CARLO SIMULATION

Let $\|x_{P1}\|, \|x_{P2}\|, \dots, \|x_{PMC}\|$ be a sequence of independent identically distributed random variables with finite mean $\|x\|$ and variance σ' (depends on M, σ, ζ). Let $\overline{\|x_P\|} = \frac{\sum_{i=1}^{MC} \|x_{Pi}\|}{MC}$ be the average of the sample. Then the C.D.F $F_n(x)$ of the random variable $Z_{MC} = \frac{\|\overline{\|x_P\|} - \|x\|}{\sigma'/\sqrt{MC}}$ converges to the standard normal C.D.F at all points x . The Central Limit Theorem states the mean of a sample is normally distributed. This distribution is regardless of the type of distribution of data, from which the samples were taken. However, this holds only if the population is significantly larger than the number of samples. The Confidence interval can be calculated as follows:

$$ci = \left(\|\overline{\|x_P\|} - z \times \frac{s}{\sqrt{MC}}, \|\overline{\|x_P\|} + z \times \frac{s}{\sqrt{MC}} \right) \quad (31)$$

where z is the statistic associated with a certain confidence interval, s is the sample standard deviation and MC is the Monte Carlo trial's number. In case of a 95% confidence interval, the z statistic equals to 1.96 approximately.

At first glimpse, there seem to be two unknowns MC and s . However, the sample deviation can be obtained by running the simulation for a number of times (a number that does not take too much time to run but is large enough for the sample standard deviation to converge reasonably well).

Rewrite (31) in it's probabilistic form.

$$\|\overline{\|x_P\|} - z \times \frac{s}{\sqrt{MC}} < \|x\| < \|\overline{\|x_P\|} + z \times \frac{s}{\sqrt{MC}} \quad (32)$$

Split the above two inequalities and rearrange:

$$z > \frac{\|\overline{\|x_P\|} - \|x\|}{\frac{s}{\sqrt{MC}}} \quad (33)$$

$$z < -\frac{\|\overline{\|x_P\|} - \|x\|}{\frac{s}{\sqrt{MC}}}$$

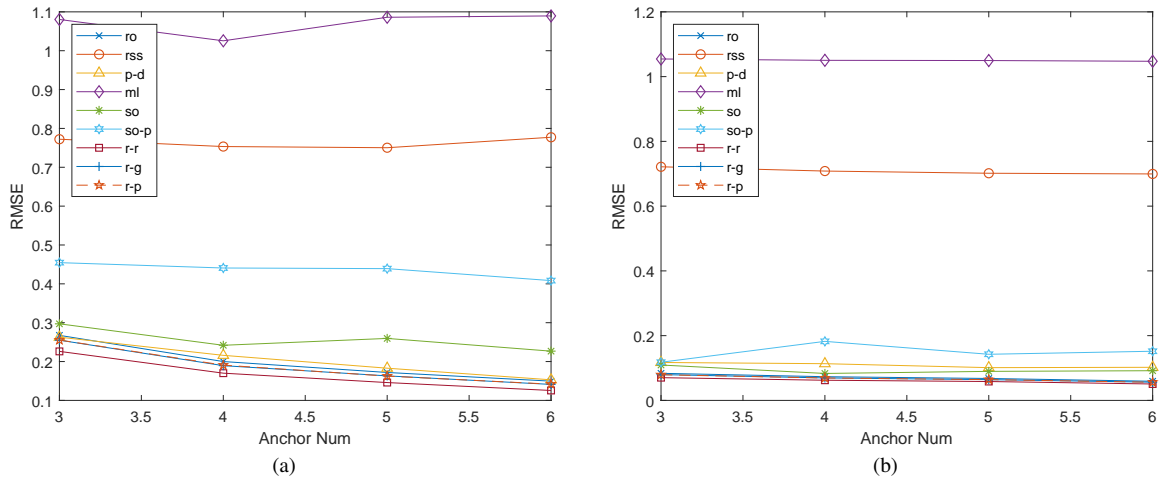


Fig. 5. Numerical simulation results of different methods with various number of anchors M . ($\zeta = 0.08$, $\sigma = 2$). (a) is "RMSE Versus M " plot under 'bad' anchor placement as shown in Fig.2a. (b) is under 'good' anchor placement as show in Fig.2b.

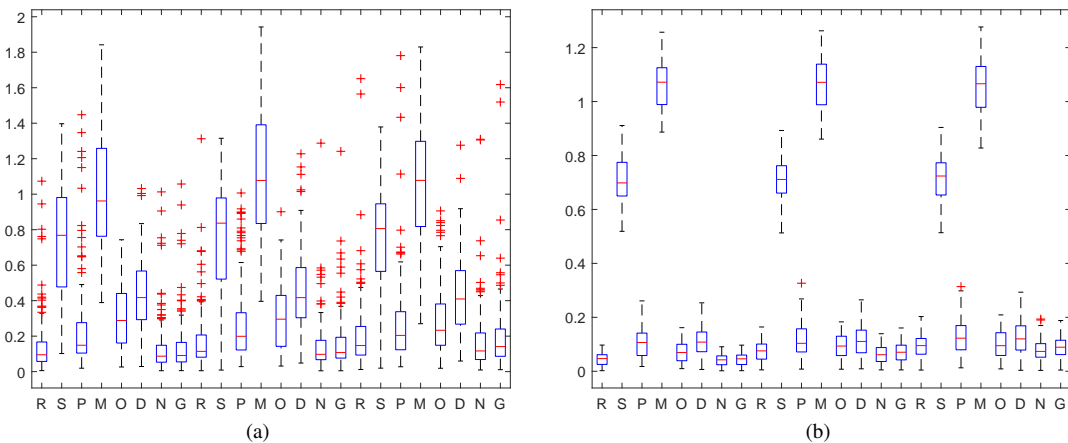


Fig. 6. The boxplot of estimation errors. (a) is under 'bad' anchor placement as shown in Fig.2a. (b) is under 'good' anchor placement as show in Fig.2b. In this subplot's x-axis label, 'R', 'S', 'P', 'M', 'O', 'D', 'N', 'G' stand for 'ro', 'rss', 'p-d', 'ml', 'so', 'so-p', 'r-r', 'r-g' respectively. All of the following figures have the same notations. In x-axis, the first group from 'R' to 'G' corresponding to $\zeta = 0.06$, the second group corresponding to $\zeta = 0.10$, and the third group corresponding to $\zeta = 0.12$.

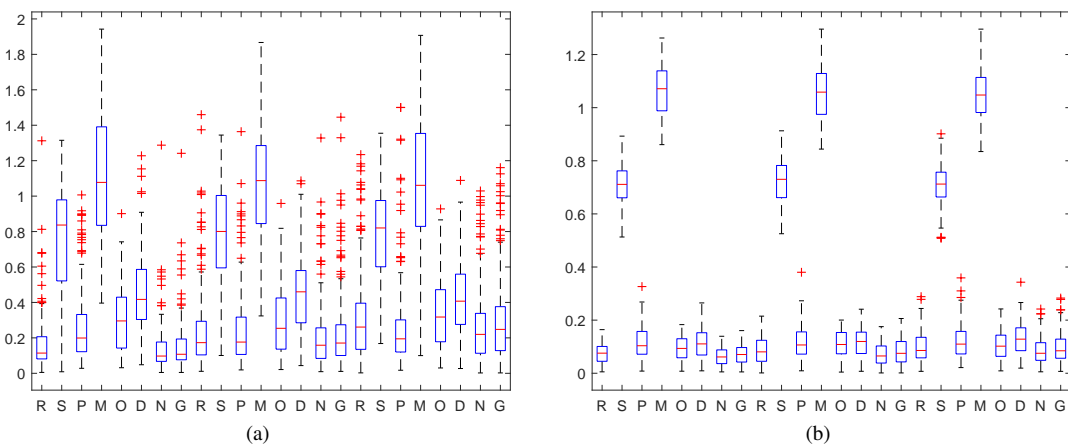


Fig. 7. The boxplot of estimation errors corresponding with different level of noise. $\zeta = 0.06$, $M = 3$. (a) is under 'bad' anchor placement as shown in Fig.2a. (b) is under 'good' anchor placement as show in Fig.2b. In x-axis, the first group from 'R' to 'G' corresponding to $\sigma = 0$, the second group corresponding to $\sigma = 2$, and the third group corresponding to $\sigma = 4$.

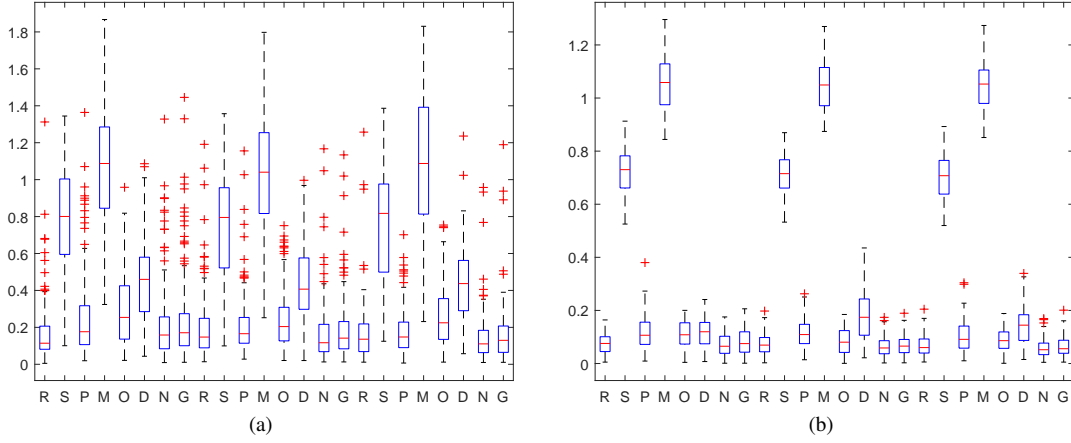


Fig. 8. The boxplot of estimation errors corresponding with different number of anchors. (a) is under 'bad' anchor placement as shown in Fig.2a. (b) is under 'good' anchor placement as show in Fig.2b. In x-axis, the first group from 'R' to 'G' corresponding to $M = 3$, the second group corresponding to $M = 4$, and the third group corresponding to $M = 5$.

Note that z is the random normal variable. Rewrite z in terms of our level of precision Φ , and then we obtain the following equation in probabilistic form:

$$P\left(-\frac{\Phi}{\frac{s}{\sqrt{MC}}} < \frac{\|x_P\| - \|x\|}{\frac{s}{\sqrt{MC}}} < \frac{\Phi}{\frac{s}{\sqrt{MC}}}\right) \quad (34)$$

If sample data are typically distributed, then the variance follows Chi-Square distribution. The distribution changes as sample size increases. For non-normal random variables, the distribution of sample variance is unknown. Because of this technical bottleneck, the technique presented here only serves the need for estimating the number of trials that are needed to achieve a certain desired level of precision. This method, however, does not produce a theoretical minimum number of the simulations needed. Nevertheless, as the sample size increases, the distribution of sample variance approaches to the normal distribution.

Here we set the level of precision at Φ . In order to calculate the required number of trials for this level of precision, the following steps should be followed:

- 1) Run the simulation 20 times, and calculate the sample standard deviation s .
- 2) Choose the confidence level and select the associated z statistic. This paper will use 95% for example and 1.96 for the z statistic.
- 3) Solve the equation $\frac{\Phi}{\frac{s}{\sqrt{MC}}} = 1.96$
- 4) Return the simulation for approximately MC times to achieve the desired level of precision.

APPENDIX B CRAMER RAO LOWER BOUND ANALYSIS

The CRLB can provide a benchmark against which we can compare the performance of the mentioned unbiased estimator.

Here we present the CRLB on the RMSE for the proposed unbiased estimator. It sets a lower limit on the co-variance matrix of any unbiased estimator. That is

$$C_{\hat{x}} = \mathbb{E}[(\hat{x} - x)(\hat{x} - x)^T] \succeq \text{CRLB} = I^{-1}(x) \quad (35)$$

where I is the Fisher information matrix

$$[I(x)]_{ij} = -\mathbb{E}\left[\frac{\partial^2 \ln p(L|x)}{\partial x_i \partial x_j}\right] \quad (36)$$

where $p(L|x)$ is the joint conditional PDF of the observation vector L given x . From (2) and (3) we know

$$L_i = L_0 + 10\gamma \log_{10} \frac{\|x - z_i - \Delta_i\|}{d_0} + m_i \quad (37)$$

In this paper we do not need to assume the distribution of Δ_i in advance. But here it is necessary to know it in advance in order to calculate CRLB. In the most general case, we assume that Δ_i is two-dimensional uniformly distributed. Its density function is

$$f(\Delta_{ix}, \Delta_{iy}) = \begin{cases} \frac{1}{\pi\zeta^2} & \|\Delta_i\| \leq \zeta \\ 0 & \|\Delta_i\| > \zeta \end{cases} \quad (38)$$

From (37), we get

$$L_i = (L_0 - 10\gamma \log_{10} d_0) + 5\gamma \log_{10} \|x - z_i - \Delta_i\| + m_i \quad (39)$$

For simplicity, let $Y_i = 5\gamma \log_{10} \|x - z_i - \Delta_i\|$, then

$$\begin{aligned} F(y_i) &= P(Y_i \leq y_i) \\ &= \int \int_{\|\Delta_i\| \leq \zeta, Y_i \leq y_i} f(\Delta_{ix}, \Delta_{iy}) d\Delta_{ix} d\Delta_{iy} \end{aligned} \quad (40)$$

Let $R_i = 10^{\frac{y_i}{10\gamma}}$, $s_i = \frac{1}{2}(\zeta + \|x - z_i\| + R_i)$ and $S = \sqrt{s_i(s_i - \zeta)(s_i - \|x - z_i\|)(s_i - R_i)}$. At first we have

$$\begin{aligned} \alpha_i &= \arccos\left(\frac{\zeta^2 + \|x - z_i\|^2 - R_i^2}{2\zeta\|x - z_i\|}\right) \\ \beta_i &= \arccos\left(\frac{R_i^2 + \|x - z_i\|^2 - \zeta^2}{2R_i\|x - z_i\|}\right) \end{aligned} \quad (41)$$

Then

$$F(y_i) = \begin{cases} 0 & \|x - z_i\| \geq R_i + \zeta \\ \frac{1}{\pi\zeta^2}(\alpha_i\zeta^2 - \beta_i R_i^2 - 2S_i) & \|x - z_i\| < R_i + \zeta \end{cases} \quad (42)$$

So the PDF of Y is

$$f(y_i) = \begin{cases} 0 & \text{when } y_i \leq 10\gamma \log_{10}(|x - z_i| - \zeta) \\ \frac{1}{\pi\zeta^2}(\alpha'_i\zeta^2 - (\beta'_i R'_i{}^2 + 2\beta_i R_i R'_i) - 2S'_i) & \text{otherwise} \end{cases} \quad (43)$$

where $R'_i = \ln 10 \frac{y_i}{10\gamma}$, and

$$\alpha'_i = \frac{2R_i R'_i}{\sqrt{(1 - (\frac{\zeta^2 + |x - z_i|^2 - R_i^2}{2\zeta|x - z_i|})^2)}} \quad (44)$$

$$\beta'_i = \frac{-\left(\frac{R'_i}{2|x - z_i|} + \frac{\zeta^2 - |x - z_i|}{2R_i^2|x - z_i|}\right)}{\sqrt{1 - \left(\frac{\zeta^2 + |x - z_i|^2 - R_i^2}{2\zeta|x - z_i|}\right)^2}}$$

Now, the density function of L_i is the convolution of $f_{Y_i}(y_i)$ and f_{m_i}

$$f(L_i) = \int_{-\infty}^{\infty} f_Y(l_i - x) \frac{1}{\sqrt{2\pi\sigma}} e^{-\frac{x^2}{2\sigma^2}} dx \quad (45)$$

Then joint conditional PDF of the observation vector L , given x is

$$p(L|x) = \prod_{i=1}^M f(L_i) \quad (46)$$

REFERENCES

- [1] E. Xu, Z. Ding, and S. Dasgupta, "Source localization in wireless sensor networks from signal time-of-arrival measurements," *IEEE Transactions on Signal Processing*, vol. 59, no. 6, pp. 2887–2897, 2011.
- [2] S. Gezici, Z. Tian, G. B. Giannakis, H. Kobayashi, A. F. Molisch, H. V. Poor, and Z. Sahinoglu, "Localization via ultra-wideband radios," *IEEE Signal Processing Magazine*, vol. 22, no. 4, pp. 70–84, 2005.
- [3] Q. Liang and S. W. Sann, "Uav-based passive geolocation based on channel estimation," in *2010 IEEE Globecom Workshops*, Dec 2010, pp. 1821–1825.
- [4] M. Rosi, M. Simie, and P. Luki, "Tdoa approach for target localization based on improved genetic algorithm," in *2016 24th Telecommunications Forum (TELFOR)*, Nov 2016, pp. 1–4.
- [5] M. Abd El Aziz, "Source localization using tdoa and fdoa measurements based on modified cuckoo search algorithm," *Wireless Networks*, vol. 23, no. 2, pp. 487–495, 2017.
- [6] W. Wang, G. Wang, F. Zhang, and Y. Li, "Second-order cone relaxation for tdoa-based localization under mixed los/nlos conditions," *IEEE Signal Processing Letters*, vol. 23, no. 12, pp. 1872–1876, 2016.
- [7] A. Canclini and F. Antonacci, "Distributed 3d source localization from 2d doa measurements using multiple linear arrays," *Wireless Communications and Mobile Computing*, 2017.
- [8] R. Levorato and E. Pagello, "Doa acoustic source localization in mobile robot sensor networks," in *2015 IEEE International Conference on Autonomous Robot Systems and Competitions*, April 2015, pp. 71–76.
- [9] J. Werner and J. Wang, "Sectorized antenna-based doa estimation and localization: Advanced algorithms and measurements," *IEEE Journal on Selected Areas in Communications*, vol. 33, no. 11, pp. 2272–2286, 2015.
- [10] Y. Zhang and S. Xing, "Rss-based localization in wsns using gaussian mixture model via semidefinite relaxation," *IEEE Communications Letters*, vol. 21, no. 6, pp. 1329–1332, 2017.
- [11] S. Tomic and M. Beko, "Distributed algorithm for target localization in wireless sensor networks using rss and aoa measurements," *Pervasive and Mobile Computing*, vol. 37, pp. 63–77, 2017.
- [12] Y. Liu, J. Chen, and Y.-j. Zhan, "Local patches alignment embedding based localization for wireless sensor networks," *Wireless personal communications*, vol. 70, no. 1, pp. 373–389, 2013.
- [13] J. Chen and Y. Liu, "Wireless sensor network localization based on semi-supervised local subspace alignment," in *Applied Mechanics and Materials*, vol. 385, 2013, pp. 1618–1621.
- [14] P. Tseng, "Second-order cone programming relaxation of sensor network localization," *SIAM Journal On Optimization*, vol. 18, no. 1, pp. 156–185, 2007.
- [15] G. Naddafzadeh-Shirazi, M. B. Shenouda, and L. Lampe, "Second Order Cone Programming for Sensor Network Localization with Anchor Position Uncertainty," *IEEE Transactions On Wireless Communications*, vol. 13, no. 2, pp. 749–763, FEB 2014.
- [16] Y. Hu and G. Leus, "Robust differential received signal strength-based localization," *IEEE Transactions on Signal Processing*, vol. 65, no. 12, pp. 3261–3276, 2017.
- [17] K. Yang, G. Wang, and Z.-Q. Luo, "Efficient convex relaxation methods for robust target localization by a sensor network using time differences of arrivals," *IEEE Transactions on Signal Processing*, vol. 57, no. 7, pp. 2775–2784, 2009.
- [18] K. C. Ho and X. N. Lu, "Source localization using tdoa and fdoa measurements in the presence of receiver location errors: Analysis and solution," *IEEE Transactions on Signal Processing*, vol. 55, no. 2, pp. 684–696, 2007.
- [19] D. E. Manolakis and M. E. Cox, "Effect in range difference position estimation due to stations' position errors," *IEEE Transactions on Aerospace and Electronic Systems*, vol. 34, no. 1, pp. 329–334, 1998.
- [20] B.-S. C. Wei-Yu Chiu, "Robust relative location estimation in wireless sensor networks with inexact position problems," *IEEE Transactions on Mobile Computing*, vol. 11, no. 6, pp. 935–946, 2012.
- [21] H. Lohrasbipeydeh and T. A. Gulliver, "Unknown RSSD-Based Localization CRLB Analysis With Semidefinite Programming," *IEEE Transactions On Communications*, vol. 67, no. 5, pp. 3791–3805, MAY 2019.
- [22] X. Wu, X. Zhu, S. Wang, and L. Mo, "Cooperative motion parameter estimation using RSS measurements in robotic sensor networks," *Journal Of Network and Computer Applications*, vol. 136, pp. 57–70, JUN 2019.
- [23] A. Goldsmith, *Wireless Communications*. Cambridge University Press, 2005.
- [24] M. Grant and S. Boyd, "CVX: Matlab software for disciplined convex programming, version 2.1," <http://cvxr.com/cvx>, Mar. 2014.
- [25] R. H. Tütüncü, K. C. Toh, and M. J. Todd, "Solving semidefinite-quadratic-linear programs using sdpt3," *Mathematical Programming*, vol. 95, no. 2, pp. 189–217, Feb 2003.
- [26] N. Patwari and A. Hero, "Relative location estimation in wireless sensor networks," *IEEE Transactions On Signal Processing*, vol. 51, no. 8, pp. 2137–2148, AUG 2003.
- [27] R. W. Ouyang and A. K.-S. Wong, "Received Signal Strength-Based Wireless Localization via Semidefinite Programming: Noncooperative and Cooperative Schemes," *IEEE Transactions On Vehicular Technology*, vol. 59, no. 3, pp. 1307–1318, MAR 2010.
- [28] X. Li and J. He, "The effect of multipath and nlos on toa ranging error and energy based on uwband," in *2016 IEEE International Conference on Consumer Electronics-Taiwan (ICCE-TW)*, May 2016, pp. 1–2.
- [29] "https://www.ibm.com/analytics/cplex-optimizer."
- [30] M. Naraghi-Pour and G. C. Rojas, "A novel algorithm for distributed localization in wireless sensor networks," *ACM Transaction on Sensor Networks*, vol. 11, no. 9, pp. 1–25, Sep. 2014.
- [31] W. Kim and M. S. Stankovic, "A distributed support vector machine learning over wireless sensor networks," *IEEE Transactions on Cybernetics*, vol. 45, no. 11, pp. 2599–2611, Nov. 2015.
- [32] C. Zhang and Y. Wang, "Distributed event localization via alternating direction method of multipliers," *IEEE Transactions on Mobile Computing*, vol. 17, no. 2, pp. 348–361, Feb. 2018.
- [33] R. Wang, B. Shen, and Y. Liu, "Optimization of sensor deployment for localization accuracy improvement," in *2016 IEEE International Conference on Consumer Electronics-China (ICCE-China)*, 2017.